Chaotic Behaviour in On-Chip Automatic Tuning Loops for Continuous–Time Filters

Herminio Martínez-García
Department of Electronics Engineering
BarcelonaTech, UPC
C/ Comte d'Urgell, 187. Campus d'Urgell
E-08016 Barcelona, Spain
herminio.martinez@upc.edu

Abdelali El Aroudi
Department of Electronics, Electrical Engineering and Automatic Control
Universitat Rovira i Virgili
Tarragona, Spain
abdelali.elaroudi@urv.cat

Eduard Alarcon, Alberto Poveda
Department of Electronics Engineering
BarcelonaTech, UPC
C/ Gran Capitán, s/n. Campus Nord
E-08034 Barcelona, Spain
{ eduard.alarcon; alberto.poveda }@upc.edu

***Abstract*—Continuous-time filters (CTF) with automatic tuning loops are nonlinear feedback systems with potential instability. While an appropriate small signal linear dynamic modeling of the tunable filter should be obtained for design purpose, its ability to predict the real nonlinear dynamic behavior of the system is limited. In order to overcome this problem, a general and systematic procedure is used to obtain a large signal nonlinear model. The obtained model can accurately predict nonlinear phenomena such as bifurcations and chaotic behavior. From this model, some numerical simulations results are presented in this paper. As far as the authors know, the observation of these phenomena in CTF with tuning loops has not been previously presented. Thus, the results obtained in this work can provide some help to obtain improved controllers (with higher bandwidth and better performance) for the two involved control loops.**

I. INTRODUCTION

Filters with tuning capabilities are adaptive filtering stages that incorporate tuning input signals aimed to directly modify the parameters of the original circuit structure. They typically exhibit a non-linearity of the bilinear type, which is well-known in several system modeling such as switching power electronics converters [1]. This bilinear behavior is due to terms containing the product of state variables and control inputs in the equations that describe their behavior. An additional source of modeling complexity of filters with tuning capability is due to the time-varying nature of the reference input signal to the control loops, which make the system prone to exhibit nonlinear phenomena that can not be predicted by a design-oriented small signal modeling approach. The prediction of such behaviors can only be predicted by a suitable model that retains the nonlinearity and the time-variance of the system.

Our purpose in this work is to propose a nonlinear dynamical model that can cope with the observed nonlinear behaviour of a continuous-time filter (CTF) with automatic tuning loops which uses a master-slave strategy. From this model, the dynamic behaviour of the system is obtained using numerical simulations. It is found that as a control parameter is varied, the system can present different kind of dynamical nonlinear behaviours that cannot be predicted by the small signal design-oriented model. The rest of the paper is organized as follows. Section II presents the system description. In section III, the mathematical dynamic model of the power plant is derived. Section IV presents the description of the control loops and their corresponding dynamical models in the Laplace and the time domain. Numerical simulations are presented in Section V, in which different bifurcation behaviours are observed. Different tools are combined to identify the dynamical behaviour of the system. Finally, some concluding remarks are drawn in the last section.

II. SYSTEM DESCRIPTION

Figure 1 shows the basic block diagram of an on-chip tuning system for a CTF which uses a typical master-slave strategy [2]-[4]. In this strategy, on the one hand, the slave filter performs the filtering process for the incoming signal. On the other, the master filter, which is embedded in the quality factor Q and central frequency ω_O tuning control loops, received the reference sinusoidal signal $v_{REF}(t)=A_{REF}\cdot\sin(\omega_{REF}t)$ as input. The frequency of this signal (which should be as stable as possible) should be tracked by the central frequency of the filter. The ω_O control loop compares the master filter's response with the reference signal $v_{REF}(t)$. This comparison generates, after filtering, a low frequency control signal $v_{CF}(t)$ that is directly proportional to the difference between the actual central frequency of the filter and the reference frequency. The control signal $v_{CF}(t)$ is in turn applied to both the master and the slave filters.

A second loop tunes the quality factor Q taking advantage of the fact that the band-pass filter gain at the central frequency is proportional to its quality factor so that its control signal $v_{CQ}(t)$ can be generated. This control signal is proportional to the difference between the instantaneoous output signal amplitude and the reference amplitude. As a particular example of the general and systematic method presented in previous section, a MOSFET-C filter is considered in this work (Fig. 1) [5]. This circuit structure consists on a state-variable filter, in particular, the so-called TQE (Transimpedance Q-Enhancement) filter [6]. In order to perform the automatic tuning of the CTF, resistors must be implemented by means of electronically tunable circuits. Among the available circuit structures, the cell known as MOS Resistive Circuit (MRC) [7], [8] is considered in this work.

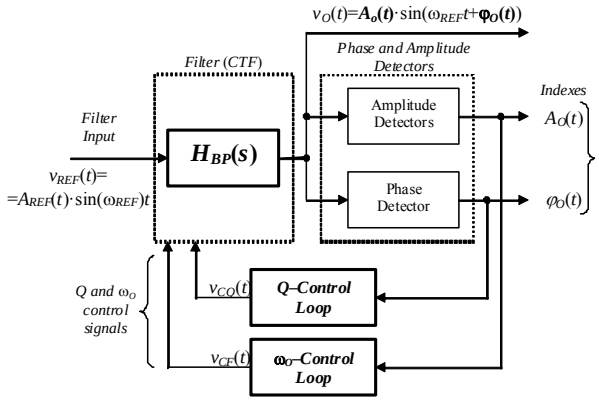

Figure 1. (*a*) Basic block diagram of an on–chip tuning system for a CTF. (*b*) Model of the CTF with the amplitude and phase detectors and control loops.

Starting from the modelling technique proposed in [2], [9] for filters with automatic tuning, the corresponding transfer functions from the quality factor control signal to the amplitude of the output signal, as well as from the central frequency control signal to the phase-shift of the output signal can be derived. As a result, these transfer functions allow to design both enhanced non-adaptive and adaptive controllers that improve the performance of previous controllers based on dominant pole compensation for tuning the quality factor (Q) and central frequency (ω_O). The aim of the self-tuning subsystem might consist not only in correcting component tolerances and drift DC errors, but also in dynamically varying Q and ω_O parameters of the CTF. An accurate dynamic model is imperative to study issues related to stability and predicting the real dynamic behavior of the system. While an appropriate *small signal linear dynamic modeling* of the tunable filter should be obtained for design purpose, its ability to predict the *large-signal nonlinear dynamic behavior* of the system is very limited. To overcome this problem, a general and systematic procedure is used to obtain a large signal nonlinear model.

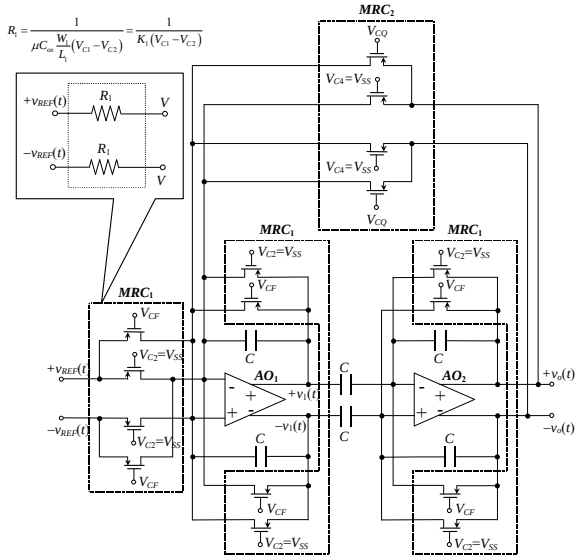

Figure 2. Transistor-level fully-balanced tunable MOSFET-C band-pass 2nd order filter.

III. Dynamic Modeling of Tunable Filters

In order to accurately predict the behavior of the tuning system, the first required step consists in modeling the filter, considered as the control system plant. Generally [3], [4], most of designed analog filtering structures including automatic tuning consider, as a master cell, second order filters with three input signals, namely: the original input signal, $v_{REF}(t)$, and two control inputs, represented as $v_{CF}(t)$ and $v_{CQ}(t)$, that tune, respectively, central frequency (ω_O) and quality factor (Q) of the filter (see Fig. 1). In addition, this second order filter has two state variables $v_1(t)$, $v_O(t)$, one of which is usually the output signal of the circuit. The system can be expressed in a space-state representation form as follows:

$$\dot{\mathbf{x}}(t)=\mathbf{A}\left(\mathbf{u}(t)\right)\cdot\mathbf{x}(t)+\mathbf{B}\left(\mathbf{u}(t)\right)\cdot v_{REF}(t)$$
$$\mathbf{x}(t)=\begin{bmatrix}v_O(t)\\ v_1(t)\end{bmatrix}\qquad \mathbf{u}(t)=\begin{bmatrix}v_{REF}(t)\\ v_{CF}(t)\\ v_{CQ}(t)\end{bmatrix}. \tag{1}$$

For the particular case considered in this work, Eq. 1 can be written more explicitly as follows:

$$\dot{\mathbf{x}}(t)=\mathbf{A}\left(v_{CF}(t),v_{CQ}(t)\right)\cdot\mathbf{x}(t)+\mathbf{B}\left(v_{CF}(t),v_{CQ}(t)\right)\cdot v_{REF}(t)\,, \tag{2}$$

where the matrices involved in (2) are given by:

$$\mathbf{A}=\begin{pmatrix}\frac{K_2}{C}v_{CQ}-\frac{K_1}{C}v_{CF} & \frac{K_2}{C}v_{CQ}\\ -\frac{K_2}{C}v_{CQ} & -\frac{K_1}{C}v_{CF}\end{pmatrix},\quad \mathbf{B}=\begin{pmatrix}\frac{K_1}{C}v_{CF}\\ -\frac{K_1}{C}v_{CF}\end{pmatrix} \tag{3}$$

In a similar way that for a typical control system, the small-signal linearised incremental model can be obtained [2], [9]. However, unlike classical control systems, in which input reference signals have constant steady-state values, the input signal processed by the CTF (and, in turn, their state variables) is sinusoidal. Besides the bilinearity that the filter exhibits due to its intrinsic adaptive behavior, the particular nature of the input signal as a sinusoidal tone requires an averaged dynamic model to be obtained for the baseband information (slow dynamics changes in envelope and phase).

From the baseband-equivalent linear equations, the transfer function that relates the amplitude of the state variables to the control voltage that tunes the quality factor $\tilde{v}_{CQ}(t)$, as well as the transfer function that relates the phase-shift of these state variables to the control voltage $\tilde{v}_{CF}(t)$ that tunes the central frequency ω_O of the master (and thus slave) filter can be obtained [2]. These transfer functions allows to obtain improved controllers for the two involved control loops, as is presented in [9].

IV. Quality Factor and Central Frequency Tuning Control Loop Scheme

The conventional tuning strategy consists of an indirect adjustment based on the so-called master-slave scheme [3]. The main filter (slave circuit) performs the filtering process for the incoming signal. The master filter, which is embedded

within the ω_O and Q tuning control loops, receives at its input the reference sinewave $v_{REF}(t)$, whose frequency should ideally be tracked by the filter, hence *indirectly* setting the central frequency of the slave filter.

A. Quality Factor Controller

A common choice for controlling the quality factor with a zero static error and a high loop bandwidth is by using a compensator with a single pole at the origin [10]. However, it has been shown in [9] that significant improvements on the system response can be achieved if a more advanced controller is used. In this paper the same controller proposed in [9] will be used. The transfer function of this controller is given by:

$$H_{CQ}(s) = \frac{K_i(s/\omega_z + 1)}{s(s/\omega_p + 1)}, \tag{4}$$

where the parameter K_i is the controller gain, and ω_z and ω_p are additional zero and pole, respectively. The input to this controller is the error signal formed between the signals $v_O^2(t)$ and $Q^2 v_{REF}^2(t)$. This error signal is then processed through the controller (4) to provide the control signal $v_{CQ}(t)$. Let this error signal be $e_{QR}(t)$. The time-domain differential equation corresponding to the signal $v_{CQ}(t)$ is given by

$$(1/\omega_p)\ddot{v}_{CQ}(t) + v_{CQ}(t) = K_i\left[(1/\omega_z)\dot{e}_{QR}(t) + e_{QR}(t)\right] \tag{5}$$

This second order equation can be further written as a set of two first order differential equations. Let us define $\dot{v}_{CQ}(t) = z(t)$. Then $\ddot{v}_{CQ}(t) = \dot{z}(t)$ and (5) becomes:

$$\begin{aligned} \dot{v}_{CQ}(t) &= z_1(t) \\ \dot{z}_1(t) &= -\omega_p v_{CQ}(t) + K_i\omega_p\left[(1/\omega_z)\dot{e}_{QR}(t) + e_{QR}(t)\right] \end{aligned} \tag{6}$$

An error signal is formed between $v_{CQ}(t)$ and a desired setpoint (zero in this case) and then it is passed through a saturation block that limits the error between 0 and 1.1 and then it is applied to the plant according to the model given in (2)-(3).

B. Central Frequency Controller

In this case the control signal $v_{CF}(t)$ is produced at the output of a controller which consists of a comparator that detect the sign of the product $v_{CF}(t)$ and $v_o(t)$. The result of the comparison is then multiplied by the reference signal $v_{REF}(t)$ and the product is then passed through an integrator. Therefore, the time-domain differential equation corresponding to the signal $v_{CF}(t)$ is given by:

$$\dot{v}_{CF}(t) = -Gv_{ref}(t)\,\mathrm{sgn}\left[\int_0^t \left(v_O(t)v_{CF}(t)\right)dt\right] \tag{7}$$

where G is a multiplicative gain. Let us define as $z_2(t) = \int_0^t \left(v_O(t)v_{CF}(t)\right)dt$ and therefore one has:

$$\begin{aligned} \dot{z}_2(t) &= v_O(t)v_{CF}(t) \\ \dot{v}_{CF}(t) &= -Gv_{ref}(t)\,\mathrm{sgn}\left[z_2\right] \end{aligned} \tag{8}$$

An error signal is formed between $v_{CF}(t)$ and a desired setpoint and then it is applied to the plant according to the model given in (2) and (3). These equations, together with (6) and (8), give the large signal nonlinear dynamical model of the system. In the following section, some numerical simulations will be performed using this model.

V. Characterizing Bifurcation Phenomena

The main purpose in this section is to use the dynamic model given (2) and (3) together with (6) and (8) to explore possible dynamic behaviors of the system. These equations correspond to a five-dimensional nonlinear time-varying model. As it will be shown later, the nonlinear and time-variance features of the model make it rich in nonlinear phenomena. The results will be presented in the form of time-domain waveforms, phase space, Poincaré sections, and FFT spectra.

Numerical solution of the above described model is obtained by using Matlab®-Simulink® with a fourth order Runge-Kutta algorithm and fixed step size of 1 μs which guarantee 400 samples within a driving signal period. For numerical simulations, let us consider the values of the parameters listed in Table I of the Appendix. In order to investigate the dynamic behavior of the system, let is monitor the steady state response while fixing all parameters and varying the feedback gain G as a control parameter. The system is simulated during 5000 driving signal periods. The first 4900 periods are considered as transient and the last 100 periods are considered as steady state. Figure 3 shows the different responses of the system when the control parameter G is varied. The following dynamical behaviors are observed in terms of the control parameters:

- $G=2\cdot10^4$: in this case, the system presents a stable 1-periodic orbit. As it can be observed in the time-domain waveforms, the output signal has the same period as the reference signal. The steady state trajectory in the state plane is closed curve and its Poincaré section is a single point (*fixed point*) in this plane. The FFT spectrum presents a single dominant tone at the forcing frequency.
- $G=3\cdot10^4$: in this case, the 1- periodic orbit loses its stability and a 3-periodic orbit appears. The steady state trajectory in the phase space is a curve which closes to itself each three driving periods and its Poincaré section is formed by three fixed points. This is confirmed by the FFT spectrum which has the appearance of the third subharmonic tone of the forcing frequency. A high THD can be appreciated from the time-domain waveform and the FFT spectrum.
- $G=4.5\cdot10^4$: for this value of the control parameter, the system exhibits a chaotic orbit. The output signal is no more periodic. The trajectory and its Poincaré section form a chaotic attractor in the phase space. The FFT spectrum in this case is spread on a wide frequency range although some dominant tones can be clearly identified at the third subharmonic tone and its multiple integers. In this case, the output signal undergoes a high THD as it can be appreciated from the time-domain waveform and the FFT spectrum.

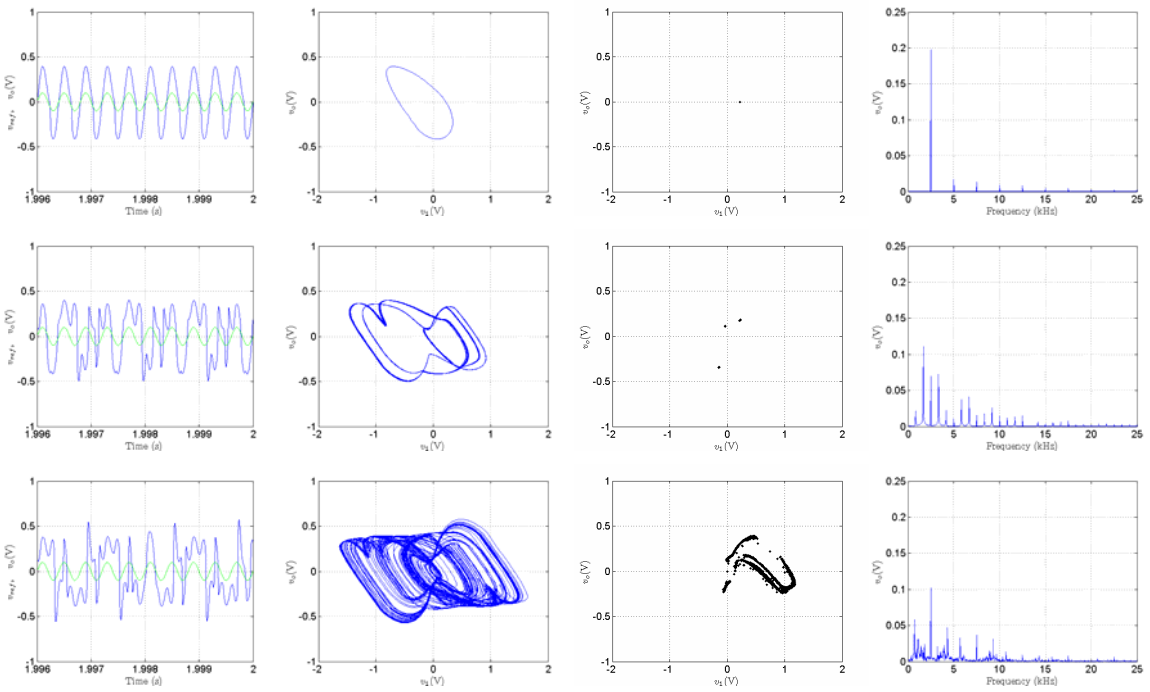

Figure 3. Steady state reponses and their corresponding state space trajectories, Poincaré sections and FFT spectra for different dynamical behaviors corresponding to different values of the control parameter. Top row: G=2·10^4 , the system exhibit a stable 1-periodic orbit. Middle row : G=3·10^4, the 1-periodic orbit.loses its stability and a stable 3-periodic orbit behavior appears. Bottom row : G=4,5·10^4, a chaotic orbit takes place.

VI. Conclusions

In this paper, we have studied the dynamic behavior of a continuous-time filter with automatic tuning loops, which is a nonlinear feedback system that can present some nonlinear phenomena. The small signal model, which is usually considered for designing the controllers, fails to predict the real behavior of the system. A large signal model is derived for the system. The obtained model can accurately predict nonlinear phenomena such as bifurcations and chaotic behavior. Finally, it is important to highlight that the results obtained in this work can provide some help to obtain improved controllers for the two involved control loops.

Acknowledgments

This work has been partially supported by the Spanish Ministry of Science and Innovation by projects TEC2010-15765, and DPI2010-16481.

References

[1] R. W. Erickson, and D. Maksimovic, Fundamentals of Power Electronics, 2nd ed., N. York: Ed. Kluwer Academic Publishers, 2001.

[2] H. Martínez, E. Vidal, E. Alarcón, and A. Poveda, "Dynamic Modeling of Analog Integrated Filters for the Stability Study of On-Chip Automatic Tuning Loops," Proceedings of the 2004 IEEE International Symposium on Circuits and Systems (ISCAS'04): pp. I-273 – I-276, 2004.

[3] R. Schaumann, M. S. Ghausi, and K.R. Laker, Design of Analog Filters. Passive, Active RC, and Switched Capacitor, Englewood Cliffs, N. Jersey: Ed. Prentice Hall, Inc., 1990.

[4] Y. P. Tsividis, and J. O. Voorman (ed.), Integrated Continuous-Time Filters: Principles, Design and Applications. A selected reprints volume. Piscataway, N. York: Ed. IEEE Press, 1993.

[5] H. Martínez, E. Vidal, E. Alarcón, and A. Poveda, "Design and Implementation of an MRC-C TQE Filter with On-Chip Automatic Tuning," Proceedings of the 44th. IEEE Midwest Symposium on Circuits and Systems (MWSCAS 2001), vol. 1, pp. 196-199, August 2001.

[6] A. Carlosena, and E. Cabral, "Novel Transimpedance Filter Topology for Instrumentation," IEEE Transactions on Instrumentation and Measurement, vol. 46 (nº 4), pp. 862–867, August 1997.

[7] Z. Czarnul. "Novel MOS Resistive Circuit for Synthesis of Fully Integrated Continuous-Time Filters," IEEE Transactions on Circuits and Systems, vol. CAS–33 (nº 7), pp. 718–721, July 1986.

[8] M. Ismail, S. V. Smith, and R. G. Beales, "A New MOSFET-C Universal Filter Structure for VLSI," IEEE Journal on Solid-State Circuits, vol. 23 (nº 1): pp. 183–194, February 1988.

[9] H. Martínez, E. Vidal, E. Alarcón, and A. Poveda, "Dynamic Modeling of Tunable Analog Integrated Filters for a Stability Study of On-Chip Automatic Tuning Loops," Analog Integrated Circuits and Signal Processing, vol. 61 (nº 3): pp. 231-246, 2009.

[10] H. Martínez, E. Vidal, A. Cantó, A. Poveda, and F. Guinjoan, "Bandwidth-Enhancement g_m-C Filter with Independent ω_O and Q Tuning Mechanisms in Both Topology and Control Loops," Proceedings of the 2010 IEEE International Symposium on Circuits and Systems (ISCAS'10): pp. 3625–3628, 2010.

Appendix

The simulations results carried out in this work have been obtained using the parameter values shown in Table I.

TABLE I. Parameter values used in the numerical simulations

K_1=383·10^{-9}	K_2=765·10^{-9}	C=5 pF	A_{REF}=0.1 V	ω_{REF}=15.7 krad/s
ω_p=2 Mrad/s	ω_z=300 rad/s	K_i=300	Q_{REF}=4	